Effect of pore size on the adsorption of xenon on mesoporous MCM-41 and on the 129Xe NMR chemical shifts: A variable temperature study

ARTICLE *in* STUDIES IN SURFACE SCIENCE AND CATALYSIS · DECEMBER 2000

DOI: 10.1016/S0167-2991(00)80253-0

6 AUTHORS, INCLUDING:

Wen-Hua Chen
Institute of Nuclear Energy Research
46 PUBLICATIONS **1,308** CITATIONS
SEE PROFILE

Hong-Ping Lin
National Cheng Kung University
143 PUBLICATIONS **3,856** CITATIONS
SEE PROFILE

Sung-Jeng Jong
Industrial Technology Research Institute
8 PUBLICATIONS **178** CITATIONS
SEE PROFILE

Shang-Bin Liu
Academia Sinica
163 PUBLICATIONS **3,568** CITATIONS
SEE PROFILE

Studies in Surface Science and Catalysis 129
A. Sayari et al. (Editors)

Effect of pore size on the adsorption of xenon on mesoporous MCM-41 and on the ^{129}Xe NMR chemical shifts: a variable temperature study

Wen-Hua Chen,[a] Hong-Ping Lin,[a] Jin-Fu Wu,[a] Sung-Jeng Jong,[a,†]
Chung-Yuan Mou[b] and Shang-Bin Liu[a,*]

[a]Institute of Atomic and Molecular Sciences, Academia Sinica,
P. O. Box 23-166, Taipei, Taiwan 106, R.O.C.

[b]Department of Chemistry, National Taiwan University, Taipei,
Taiwan 106, R.O.C.

A comprehensive study of the effect of pore size on the adsorption of xenon on mesoporous MCM-41 molecular sieves and ^{129}Xe NMR chemical shifts has been made. ^{129}Xe NMR spectra of MCM-41 samples (Si/Al = 37; pore size 1.8-3.0 nm) with varied xenon loading were obtained at different temperatures (140-340 K). The observed ^{129}Xe NMR chemical shifts were fitted by regressional nonlinear least-squares fitting based on a two-site exchange model. As a result, the temperature variation of ^{129}Xe chemical shifts at zero xenon loading, i.e. $\delta_s(\rho = 0)$ which arise mainly from xenon-wall interactions, were obtained. The pore size (d) and δ_s can be correlated by an empirical relations: $\delta_s(T, d) = A(T)/(d + B(T))$. The two parameters, A(T) and B(T), are found to have nearly the same temperature dependence. At low temperature (T < 190 K), the two parameters both increase abruptly with decreasing temperature. Whereas at high temperature (T > 250 K), they were found to slowly decrease with increasing temperature.

1. INTRODUCTION

The dynamics of the molecules adsorbed in confined geometry is one of the most common and important research subject which has received much attention in the past few decades. Owing to the large polarizability and the chemical inert nature of the monoatomic xenon, the ^{129}Xe NMR chemical shift is very sensitive to its environment and thus provides an ideal probe for the investigation of the structure of porous materials [1]. There have been numerous publications in this area since the pioneering works by Ito and Fraissard [2] and by Ripmeester [3], and several reviews have been attributed to related subjects [4-7]. Recent developments of the mesoporous MCM-41 materials [8] have also drawn intense attention due

[†]Present address: Union Chemical Lab, Industrial Technology Research Institute, Hsinchu, Taiwan 300, R.O.C.
[*]Corresponding author.

to their potential applications as catalysts or catalyst supports. The structure of MCM-41 consists of a hexagonal array of one-dimensional channels of uniform mesopores with pore diameter in the range 1.5-10 nm, depending on the nature of the template and synthesis conditions [9]. The straight, unconnected channels of controllable pore size make MCM-41 an ideal model adsorbent for both theoretical and experimental investigation of critical phenomena of molecules in a confined space [10-12]. ^{129}Xe NMR provides an excellent probe to investigate the morphology and topology of MCM-41. In particular, at the limit of low coverage, the interactions between a Xe atom (adsorbate) and the MCM-41 adsorbent deserve further investigation, in part, because of the amorphous nature of the wall structure which are still not well known at the present [8, 9].

It is the purpose of the present paper to study the effect of pore size on the adsorption of xenon on mesoporous MCM-41 molecular sieves. In particular, much attention will be focused on the temperature variation of ^{129}Xe NMR chemical shifts at low Xe loading to realize the characteristics of the Xe-wall interactions.

2. EXPERIMENTAL

Powdered, particulate MCM-41 molecular sieves (Si/Al = 37) with varied pore diameters (1.80, 2.18, 2.54 and 3.04 nm) were synthesized following the conventional procedure using sodium silicate, sodium aluminate and C_nTMAB (n = 12, 14, 16 and 18) as the source materials for Si, Al and quaternary ammonium surfactants, respectively [13]. Each sample was subjected to calcination in air at 560 °C for 6 h to remove the organic templates. The structure of the synthesized material was confirmed by powder X-ray diffraction (XRD) and by scanning/transmission electron microscopy. Their average pore sizes were deduced from the adsorption curve of the N_2 adsorption-desorption isotherm obtained at 77 K by means of the BJH method (Table 1).

Calcined sample (ca. 0.1 g) was first introduced into a designed sample cell then subjected to dehydration by gradual heating (1 °C min^{-1}) from room temperature (25 °C) to 350 °C for at least 40 h under vacuum. After sample dehydration, a known amount of Xe (70% ^{129}Xe isotope-enriched) was introduced into the sample and then the sample cell was sealed off with a mini-torch while Xe was trapped at the bottom of the sample cell by liquid N_2. Special cares were taken in minimizing the dead volume of each sample cell during glass sealing. For practical purposes, the amount of Xe adsorbed, ρ, is expressed as the number of Xe atoms per

Table 1
Characteristics of the MCM-41 samples

Pore Diameter (nm)	Si/Al	ΔE_{ads}(exp) (kcal/mol)[a]	ΔE_{ads}(fit) (kcal/mol)[b]	δ_{0z} (ppm)[c]
1.80	37	2.07	2.71	107
2.18	37	2.09	2.87	105
2.54	37	2.10	2.57	105
3.04	37	2.05	2.78	107

[a]Obtained from the experimental results shown in Fig. 3.
[b]Results obtained from data fittings.
[c]Obtained from data fitting by Eq. 4.

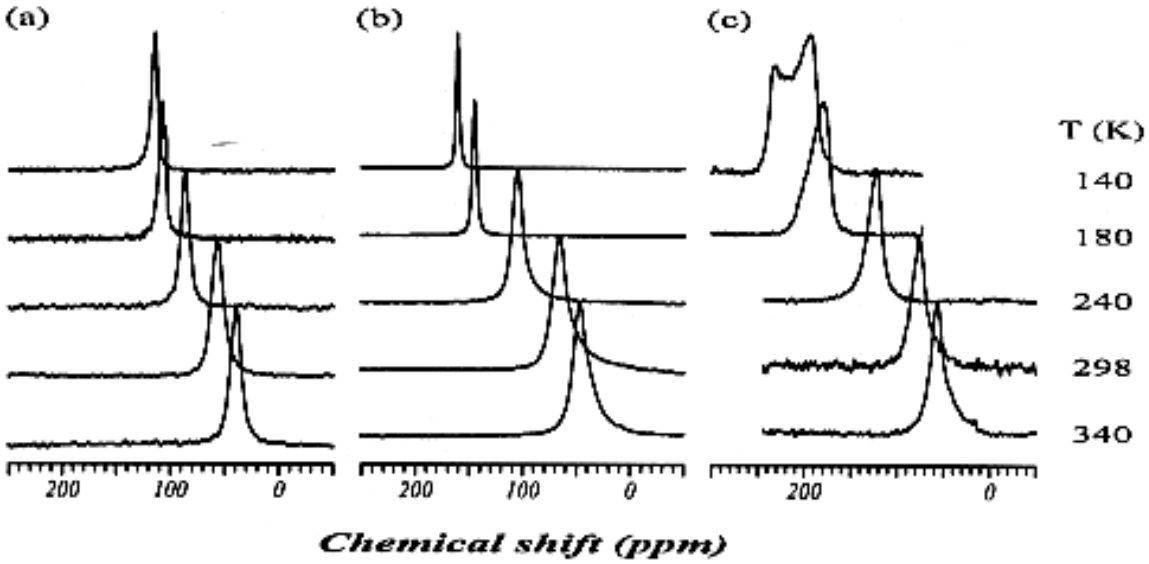

Figure 1. Temperature variations of ^{129}Xe NMR spectrum for an MCM-41 sample (pore diameter 3.04 nm) at assorted Xe loading, ρ, of (a) 12, (b) 119, and (c) 243 amagat.

effective free volume of anhydrous MCM-41 at room temperature. As a result, samples with varied Xe loading ranging from 2-245 amagat (i.e. the gas density at 0 °C and 1 atm) were prepared. One should bear in mind that the Xe loading so determined represents the *apparent* Xe density (Xe in the overall sample region). The *true* or *effective* density (Xe adsorbed within the pore of MCM-41) only when at low enough temperature to which the amount of gaseous Xe (outside of the pore) is negligible. The *effective* Xe density for each sample was calibrated by xenon adsorption isotherm done at designated temperatures (see below).

^{129}Xe NMR measurements were performed at 138.326 MHz on a Bruker MSL-500P NMR spectrometer. The free-induction-decay signals were accumulated typically with a relaxation delay of 0.3 s. All ^{129}Xe chemical shifts were referred to gaseous Xe at zero density [15]. The experimental temperatures are believed accurate to ± 2 °C. Detailed sample preparation and experimental procedures have been described in an earlier report [10].

3. RESULTS AND DISCUSSION

3.1. ^{129}Xe NMR chemical shifts: Xe-wall interactions (δ_s)

Typical ^{129}Xe NMR spectra for Xe adsorbed on MCM-41 are depicted in Fig. 1 for assorted Xe loading and temperatures. A decrease in the NMR linewidths with temperature were observed with decreasing temperature except for the high Xe loading samples at T < 190 K (Fig. 1c) which can be ascribed due to condensation of Xe within the pores of MCM-41 (*vide infra*). The additional peak at ca. 245 ppm in Fig. 1c resembles the chemical shift of bulk liquid Xe. Typical variations of ^{129}Xe chemical shift with *apparent* Xe loading are depicted in Fig. 2 for Xe adsorbed on MCM-41 with pore diameter of 2.54 nm. Similar results were found for the other MCM-41 samples with different pore sizes. To obtain the correlation between the ^{129}Xe chemical shift with *effective* Xe loading, the observed chemical shifts must be calibrated by the curves shown in Fig. 3, which were deduced from the xenon adsorption isotherms at selected temperatures. The results after such calibration are presented in Fig. 4. It

is noted that, regardless of the pore size, the curves in Fig. 3 plateau at T < 190 K indicating a complete adsorption of Xe *within* the pores of the MCM-41.

It is noted that, at low loading, the chemical shift show a parabolic-like curvature (Figs. 2 and 4). Such behavior was not found in the silica-form (Si/Al = ∞) MCM-41 sample [10] and hence may be ascribed as due to the presence of Al in the wall of MCM-41. Such parabolic-like chemical shift behavior has also been observed in amorphous alumina and silica-alumina at low Xe loading, to which Cheung *et al.* [16] ascribed as due to the presence of a broad distribution of pore sizes. MCM-41 is known, thus far, to possess partially crystalline structure analogous to amorphous silica [8]. Results obtained from our SEM/TEM and N_2 adsorption-desorption isotherm indeed indicated that, unlike the silica-form MCM-41, the Al-containing MCM-41 synthesized via the delay neutralization method [13] tends to possess an additional broad distribution of large defect cavities typically in the order of 10-20 nm. It is noted that, the existence of such pore-intersecting cavities favors the transport of the adsorbates within the hexagonal array of one-dimensional pores of MCM-41 and hence should be beneficial for use of the material as catalyst or catalyst support.

Ito and Fraissard [2] expressed the room temperature ^{129}Xe NMR chemical shift of Xe adsorbed in porous adsorbent as $\delta = \delta_o + \delta_s(\rho = 0) + \sigma_1\rho$, where $\delta_o = 0$ is the chemical shift reference, $\delta_s(\rho = 0)$ represents the interaction between a Xe atom and the wall of the adsorbent. The last term represents the contribution arising from binary Xe-Xe interactions which, at moderate loading, is linear with ρ. In the present study, the observed ^{129}Xe NMR chemical shifts can be expressed as the function of Xe loading and temperature as:

$$\delta(\rho, T) = \delta_s(T) + \sigma_1(T)\rho + \sigma_2(T)\rho^2 + \ldots. \quad (1)$$

It has been demonstrated that the temperature and density dependence of the ^{129}Xe chemical shift can be expressed as weighted average between two sites in rapid exchange [10]. That is,

$$\delta(\rho, T) = P_a(T)\delta_a(\rho_a, T) + P_g(T)\delta_g(\rho_g, T), \quad (2)$$

where P_a and P_g are the probabilities of finding the adsorbed and gaseous xenon, respectively; ρ_a and ρ_g are the density of the adsorbed and non-adsorbed Xe; $\rho = \rho_a + \rho_g$. The probability of finding a Xe atom at the wall is given by [17]: $P_a = \rho_a/\rho = \tau_a/(\tau_a + \tau_g)$; $P_g = \rho_g/\rho = 1 - P_a$, where τ_a is the average time xenon spent on the wall, and τ_g us the reciprocal of the xenon collision rate with the surface. The average xenon sticking time on the wall is given by $\tau_a = \tau_o \exp(\Delta E_{ads}/RT)$, where τ_o is the preexponential factor and ΔE_{ads} is the energy of adsorption (Table 1), and R is the gas constant. For practical purposes, we express the adsorbed and gaseous chemical shift contributions as second-order polynomials:

$$\delta_a(\rho_a, T) \approx \delta_{oa} + \sigma_{1a}(T)\rho_a + \sigma_{2a}(T)\rho_a^2; \quad \delta_g(\rho_g, T) \approx \delta_{og} + \sigma_{1g}(T)\rho_g + \sigma_{2g}(T)\rho_g^2 \quad (3)$$

The term $\delta_g(\rho_g, T)$ can be expressed explicitly according to the relation given by Jameson and co-workers [15], where $\delta_{og} = 0$ is the chemical shift reference. Here, we state without proof that the temperature dependence of the Xe-wall interaction can be explicitly expressed as [10]:

$$\delta_s(T) = P_a(T)\delta_{oa}, \quad (4)$$

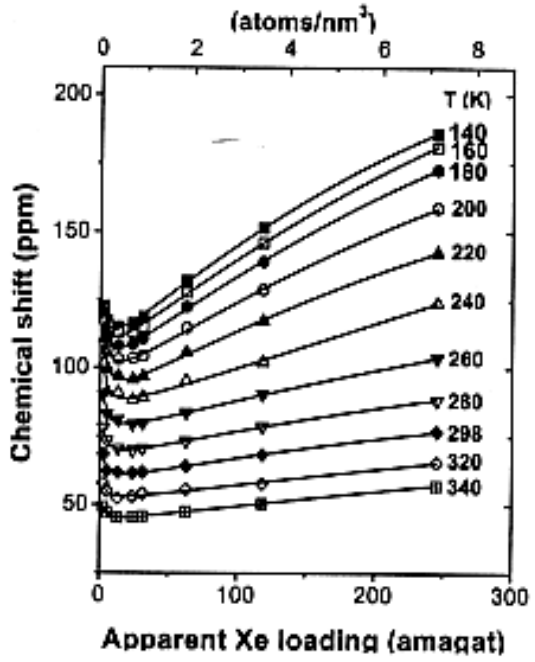

Figure 2. Variations of ^{129}Xe NMR chemical shift with *apparent* Xe loading for an MCM-41 sample (pore diameter 2.54 nm) at various temperatures.

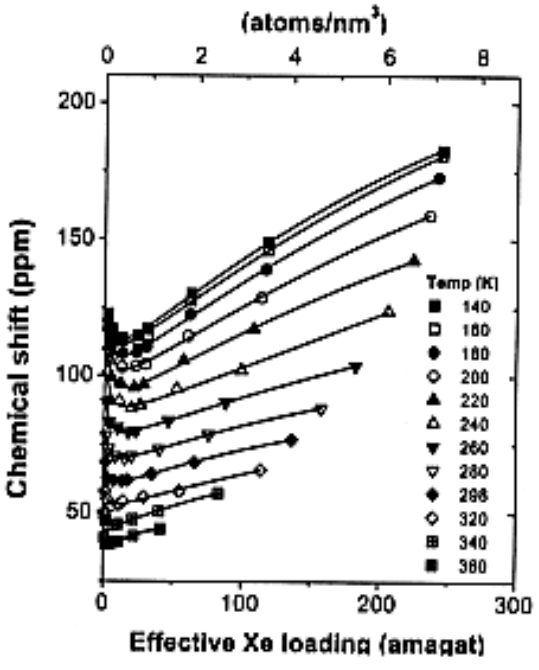

Figure 4. Variations of ^{129}Xe NMR chemical shift with *effective* Xe loading for an MCM-41 sample (pore diameter 2.54 nm) at various temperatures.

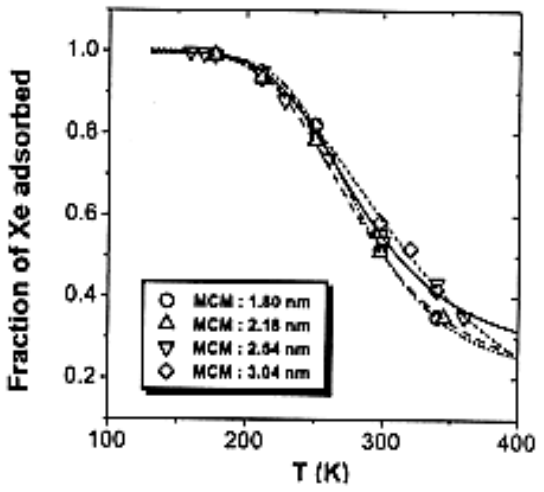

Figure 3. Plot of fraction of xenon adsorbed on MCM-41 vs. temperature for MCM-41 samples with various pore sizes.

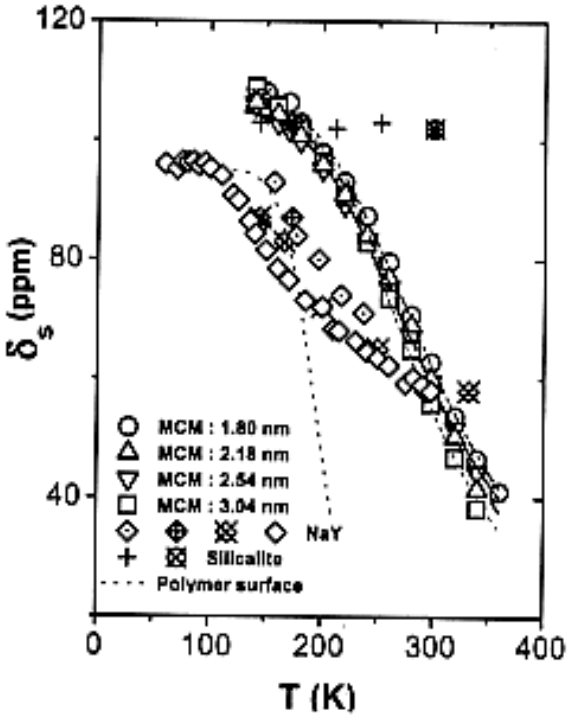

Figure 5. Temperature dependence of Xe-wall interactions for MCM-41 samples with various pore sizes. The data obtained from Xe adsorbed on silicalite (ref. 18), zeolite NaY (refs. 14, 16, 19) and on polymer surfaces (ref. 17) are also shown for comparison.

and the results of the fitting are shown in Fig. 5 together with the data obtained from Xe adsorbed on silicalite [18], microporous zeolite NaY [14, 16, 19] and polymer surface [17]. It is noted that the temperature variation for the Xe-wall interactions is nearly independent of the pore size. This is in line with the fact that all samples have the same Si/Al ratio and thus have similar structural environments near the channel walls, as experienced by the adsorbed Xe. Nonetheless, it is surprising that the averaged value of δ_{∞} ~ 106 ppm for MCM-41 is much higher than the values found for Xe adsorbed on NaY zeolite (87 ppm) [19] or on the surface of poly(acrylic acid) polymer (95 ppm) [17] but similar to that of silicalite (103 ppm) [18]. A recent molecular simulation study [20] showed that the partially crystalline structure of MCM-41 [8] possesses a high skeletal density of ca. 2.7 g cm^{-3}, which is equivalent to ca. 27 T-sites per nm^3 for solid alone and 11-19 T-sites when the pore spaces are also included. The skeletal density of MCM-41 is very close to quartz (2.66 g cm^{-3}) and is indeed substantially higher than amorphous silica (2.2 g cm^{-3}) and zeolites (typically less than 2 g cm^{-3}). Alternatively, the observed high δ_{∞} value for MCM-41 may also be ascribed due to the fact that the observed adsorption energy ΔE_{ads} (ca. 2.0 kcal/mol; Table 1) as compare to ca. 0.6 kcal/mol observed for Xe adsorbed on NaY zeolite [19]. Finally, the fact that the fitted ΔE_{ads} values (Table 1) are in good agreement with the experimental results indicates that our model gives reasonable and meaningful quantitative description of the system.

3.2. Correlation between δ_s and pore size

The correlation between δ_s and pore size obtained from different MCM-41 samples at different temperatures are shown in Fig. 6. At a given temperature T, the pore size dependence of δ_s can be described by the empirical relation:

$$\delta_s(T, d) = A(T)/(d + B(T)), \qquad (5)$$

where d is the pore diameter in nm. For comparison, the empirical relation, $\delta_s = 49.9/(d - 0.2346)$, derived by Demarquay and Fraissard [21] for Xe adsorbed in microporous zeolites (*at room temperature*) is also shown in Fig. 6. The sizable discrepancy (ca. 25 ppm) in room temperature δ_s values at 1.5 nm, the threshold pore size which distinguishes microporous from mesoporous adsorbents, is again ascribed due to the difference in their skeletal density or numbers of T-sites on the wall per unit area. The temperature variations of the two empirical parameters A(T) and B(T) are shown in Fig. 7, which show nearly the same temperature dependence. At low temperature (T < 190 K), they both increase abruptly with decreasing temperature. This is most likely due to the condensation of Xe *inside* the pore of MCM-41. Presumably, the low temperature variations of these two temperature dependent parameters can be used to deduce the phase transition properties for the adsorbed Xe. Considering the phase transition properties of bulk Xe (boiling point at 165 K; triple-point at 161.2 K), It is indicative that notable increase in these transition temperatures occurs when Xe is adsorbed within the mesoporous MCM-41.

At higher temperatures (T > 250 K), the two variables were found to slowly decrease with increasing temperature. For a more quantitative analysis of the data, we express the two parameters by simple polynomial functions:

$$A(T) = A_0 + A_1T + A_2T^2 + A_3T^3 + \ldots; \quad B(T) = B_0 + B_1T + B_2T^2 + B_3T^3 + \ldots \qquad (6)$$

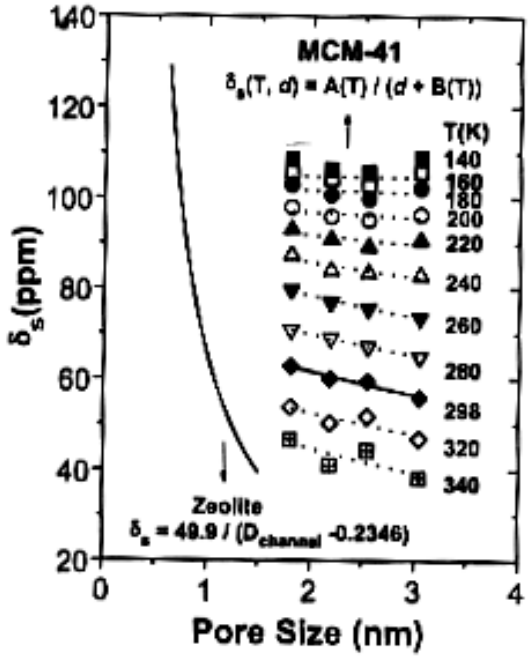

Figure 6. Variations of δ_s and pore size obtained from various MCM-41 samples at different temperatures.

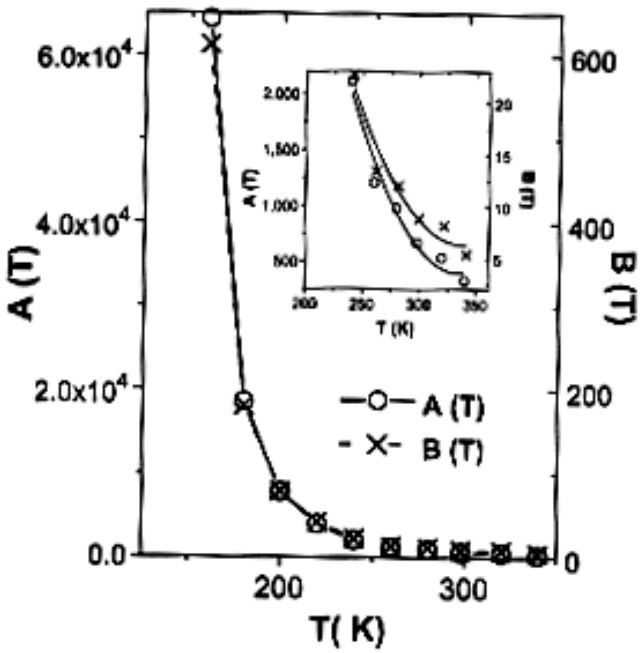

Figure 7. Temperature variations of the two constant variables A(T) and B(T) defined in Eqs. 5 and 6 (see text).

The results obtained from the regressional polynomial fittings are listed in Table 2. Such quantitative data should be helpful in estimating the value for δ_s at any temperature if the pore size of the MCM-41 is known, or *vise versa*.

Table 2
Temperature coefficients of A(T) and B(T) which correlate Xe-wall contribution of ^{129}Xe NMR chemical shift (δ_s) and the pore size of MCM-41 molecular sieves (Eq. 5)[a]

A_0	A_1	A_2	B_0	B_1	B_2
20467.67	-119.80	0.1788	189.82	-1.0904	0.00162

[a]Obtained by regressional polynomial fittings (Eq. 6) to the second order.

4. CONCLUSIONS

We demonstrate that the physical properties of Xe adsorbed in mesoporous MCM-41 molecular sieves can be deduced from the analysis of the variable temperature ^{129}Xe NMR chemical shift data. For example, the interactions between the adsorbed Xe and the wall of the adsorbent, δ_s. Our results indicate that the interactions arise from Xe adsorbed in mesoporous MCM-41 deviates significantly from not only the bulk Xe, but also from Xe adsorbed on microporous adsorbents or polymer surfaces. At a given temperature T, the pore size dependence of δ_s can be described by the empirical relation: $\delta_s(T, d) = A(T)/(d + B(T))$. The two temperature-dependence parameters were expressed by polynomial functions whose temperature coefficients were also revealed explicitly to the second order.

ACKNOWLEDGMENTS

The authors thank Profs. Soofin Cheng and Ben-Zu Wan for helpful discussions. This research has been partially supported by a grant from the Chinese Petroleum Corporation (87-S-032) and by the Nation Science Council, R. O. C. (NSC88-2113-M-001-008 to SBL).

REFERENCES

1. J. Reisse, Nouv. J. Chim., 10 (1986) 665.
2. (a) T. Ito and J. Fraissard, in: L.V.C. Rees (ed.), Proc. 5th Inter. Zeolite Conf. Heyden, London, 1980, p. 510; (b) *ibid*, J. Chem. Phys., 76 (1982) 5225.
3. (a) J.A. Ripmeester, ISMAR-Ampere Inter. Conf. on Magn. Reson., Delft, Netherlands, 1980; (b) *ibid*, J. Am. Chem. Soc., 104 (1982) 289.
4. J. Fraissard, Zeolites, 8 (1988) 350.
5. C. Dybowski, N. Bansal and T.M. Duncan, Ann. Rev. Phys. Chem., 42 (1991) 433.
6. P.J. Barrie and J. Klinowski, Progr. NMR Spectrosc., 24 (1992) 91.
7. D. Raftery and B.F. Chmelka, in: P. Diel et al. (eds.), NMR Basic Principles and Progress, Vol. 30, Springer-Verlag, Berlin, Heidelberg, 1994, p. 111.
8. (a) C.T. Kresge, M.E. Leonowicz, W.J. Roth, J.C. Vartuli and J.S. Beck, Nature, 359 (1992) 710; (b) J.S. Beck, J.C. Vartuli, W.J. Roth, M.E. Leonowicz, C.T. Kresge, K.D. Schmitt, C.T.W. Chu, D.H. Olson, E.W. Sheppard, S.B. McCullen, J.B. Higgins and J.L. Schlenker, J. Am. Chem. Soc., 114 (1992) 10834.
9. H.P. Lin, Y.R. Cheng, C.R. Lin, F.Y. Li, C.L. Chen, S.T. Wong, S. Cheng, S.B. Liu, B.Z. Wan, C.Y. Mou, C.Y. Tang and C.Y. Lin, J. Chin. Chem. Soc., 46 (1999) 495.
10. S.J. Jong, J.F. Wu, A.R. Pradhan, H.P. Lin, C.Y. Mou and S.B. Liu, Stud. Surf. Sci. Catal., 117 (1998) 543.
11. E.W. Hansen, E. Tangstad, E. Myrvold and T. Myrstad, J. Phys. Chem., 101 (1997) 10709.
12. K Morishige and K. Nobuoka, J. Chem. Phys., 107 (1997) 6965, and references therein.
13. H.P. Lin, S. Cheng and C.Y. Mou, Microporous Mater., 10 (1997) 111.
14. S.B. Liu, L.J. Ma, M.W. Lin, J.F. Wu and T.L. Chen, J. Phys. Chem., 96 (1992) 8120; J. Phys. Chem., 98 (1994) 4393.
15. C.J. Jameson, A.K. Jameson and S.M. Cohen, J. Chem. Phys., 59 (1973) 4540; J. Chem. Phys., 62 (1975) 4224.
16. T.T.P. Cheung, C.M. Fu and S. Wharry, J. Phys. Chem., 92 (1988) 5170; T.T.P. Cheung, J. Phys. Chem., 93 (1989) 7549; T.T.P. Cheung and C.M. Fu, J. Phys. Chem., 93 (1989) 3740.
17. D. Raftery, L. Reven, H. Long, A. Pines, P. Tang and J.A. Reimer, J. Phys. Chem., 97 (1993) 1649.
18. (a) Q.J. Chen and J. Fraissard, J. Phys. Chem., 96 (1992) 1809; (b) T.T.P. Cheung, J. Phys. Chem, 94 (1990) 376.
19. A. Labouriau, T. Pietrass, W.A. Weber, B.C. Gates and W.L. Earl, J. Phys. Chem. B, 103 (1999) 4323.
20. M.W. Maddox, J.P. Oliver and K.E. Gubbins, Langmuir, 13 (1997) 1737.
21. J. Demarquay and J.P. Fraissard, Chem. Phys. Lett., 136 (1987) 314.